J. Mol. Biol. (1982) **155**, 347–366

Sequential Resonance Assignments in Protein ^{1}H Nuclear Magnetic Resonance Spectra

Basic Pancreatic Trypsin Inhibitor

GERHARD WAGNER AND KURT WÜTHRICH

Institut für Molekularbiologie und Biophysik
Eidgenössische Technische Hochschule
ETH-Hönggerberg, CH-8093 Zürich
Switzerland

(Received 17 August 1981)

The assignment of the ^{1}H nuclear magnetic resonance spectrum of the basic pancreatic trypsin inhibitor with the use of two-dimensional ^{1}H nuclear magnetic resonance techniques at 500 MHz is described. The assignments are based entirely on the known amino acid sequence and the nuclear magnetic resonance data. Individual resonance assignments were obtained for all backbone and C^β protons, with the exception of those of Arg1, Pro2, Pro13 and the amide proton of Gly37. The side-chain resonance assignments are complete, with the exception of Pro2 and Pro13, the N^δ protons of Asn44 and the peripheral protons of the lysine residues and all but two of the arginine residues.

1. Introduction

The basic pancreatic trypsin inhibitor is a small globular protein of 58 amino acid residues, M_r 6500, which inhibits the function of trypsin and other proteases by formation of inert complexes with the enzymes (Tschesche, 1974). A refined crystal structure at 1·5 Å resolution has been described (Deisenhofer & Steigemann, 1975) and, during the last decade, BPTI† was the subject of a large number of experimental and theoretical studies on static and dynamic aspects of protein conformations and on protein folding. This paper describes individual ^{1}H nuclear magnetic resonance assignments for BPTI, which provide a basis for determination of the solution conformation and hence a meaningful, detailed comparison of the spatial structures of this protein in single crystals and in solution.

BPTI was previously extensively investigated by n.m.r. In particular, individual assignments obtained by a variety of different experiments (some of these depended also on reference to the crystal structure: for a survey of the original references and data, see Wüthrich & Wagner, 1979) for the eight aromatic rings, the

† Abbreviations used: BPTI, basic pancreatic trypsin inhibitor; n.m.r., nuclear magnetic resonance; p.p.m., parts per million; COSY, 2-dimensional correlated spectroscopy; NOESY, nuclear Overhauser enhancement spectroscopy; SECSY, spin echo correlated spectroscopy.

0022-2836/82/070347-20 $02.00/0

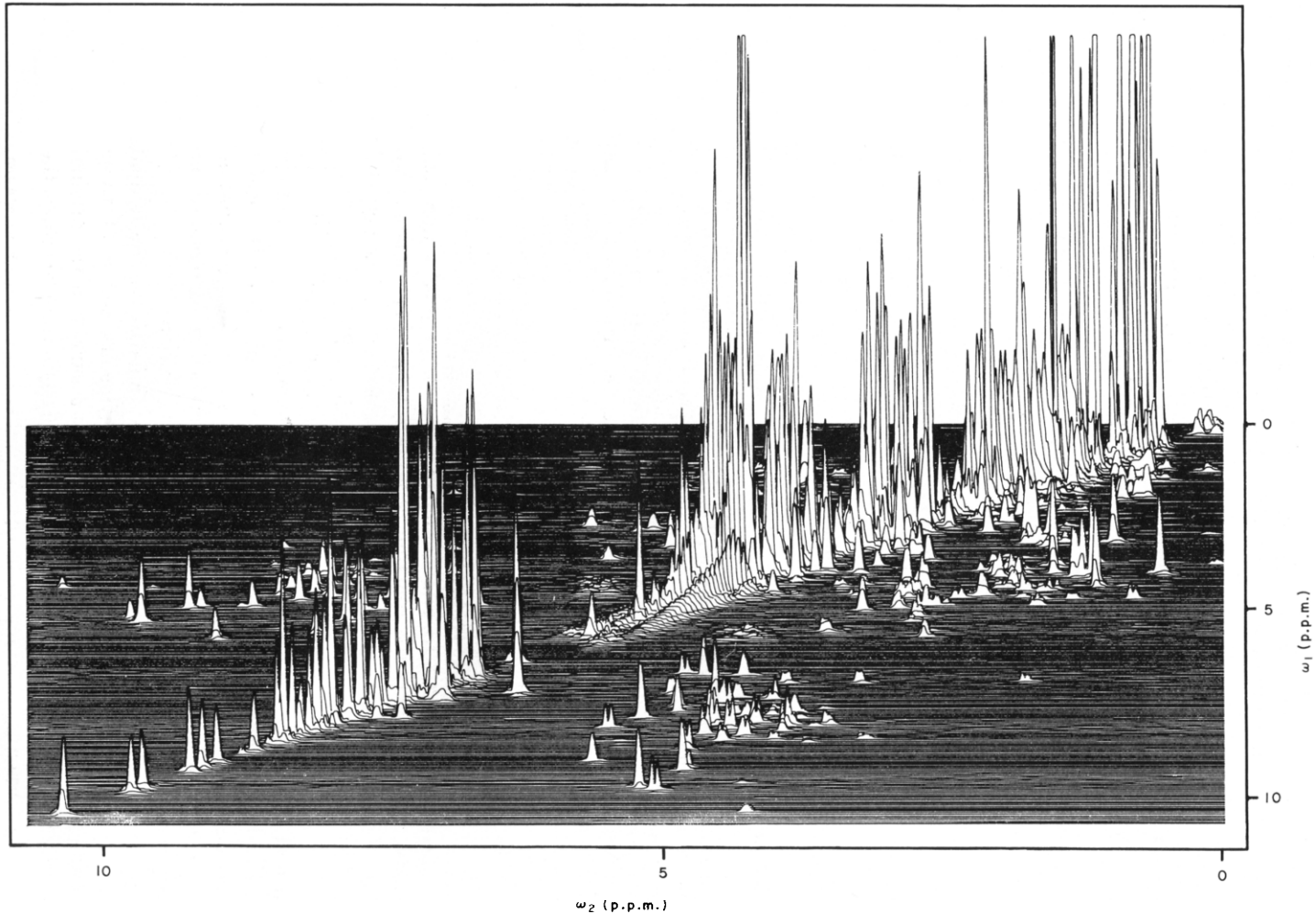

FIG. 1. Stacked-plot representation of a symmetrized (Baumann *et al.*, 1981), absolute value 500 MHz ^{1}H COSY spectrum of a 0·02 M solution of BPTI in a mixed solvent of 90% H_2O and 10% ^2H_2O, pH 4·6, $t = 80$ C. The spectrum was recorded in ~ 24 h, the digital resolution is 5·3 Hz/point. The stacked plots afford a "3-dimensional" view of the spectrum. The 2 perpendicular frequency axes ω_1 and ω_2 are calibrated with the chemical shifts. Peaks corresponding to the one-dimensional spectrum are displayed on the diagonal from the upper right to the lower left corner, where some of the highest peaks have been truncated. "Cross peaks" manifesting J connectivities between distinct lines on the diagonal are located in pairs, symmetrical with respect to the diagonal. Between 4·0 and 5·2 p.p.m., a band of artifactual peaks parallel to and in front of the diagonal spectrum are seen. These are a consequence of the water irradiation and the symmetrization of the spectrum.

20 methyl groups and selected backbone amide protons provided a basis for locating internal motions manifested in aromatic ring flips (Wüthrich & Wagner, 1975), amide proton exchange rates (Richarz *et al.*, 1979) and ^{13}C relaxation parameters (Richarz *et al.*, 1980) in specific regions of the molecule (Wagner & Wüthrich, 1979*a*; Wüthrich *et al.*, 1980). More recently, sequential resonance assignments with the use of two-dimensional n.m.r. experiments resulted in complete resonance assignments for the polypeptide segments residues 16 to 36 and 43 to 45 in the β-sheet of BPTI (Wagner *et al.*, 1981). Here, we describe sequential, individual resonance assignments for the other regions of the polypeptide chain.

2. Materials and Methods

^{1}H–^{1}H J-connectivity maps were obtained with 2-dimensional correlated spectroscopy. COSY spectra were recorded with a sequence of 2 non-selective 90° pulses (Aue *et al.*, 1976):

$$(90° - t_1 - 90° - t_2)_n.$$

The first 90° pulse creates transverse magnetization. During the evolution period, t_1, the various magnetization components precess with their characteristic precession frequency in the x–y plane of the rotating frame and are thus frequency labelled. The second 90° pulse causes transfer of magnetization components among those transitions that belong to the same J-coupled spin systems. The free-induction decay is recorded immediately after the second 90° pulse as a function of t_2. The experiment is repeated for a set of equidistant t_1 values. To obtain an adequate signal to noise ratio, n transients are accumulated for each value of t_1. At the end of each recording, the system was allowed to reach equilibrium during a fixed relaxation delay of 1 to 1·5 s.

Two-dimensional Fourier transformation of the data matrix $s(t_1, t_2)$ produced the desired frequency domain spectrum $S(\omega_1, \omega_2)$. As an illustration, Figure 1 shows a stacked-plot representation of a COSY spectrum of BPTI. The 2 perpendicular axes are calibrated with the chemical shifts, which increase from right to left and from the upper to the lower end, respectively. In this representation, peaks corresponding to the unidimensional spectrum appear on the diagonal from the upper right to the lower left of the ω_1–ω_2 plane. J-connectivities between individual lines are manifested by pairs of cross peaks in symmetrical locations with respect to the diagonal peak. A COSY spectrum can, with a single instrument setting, provide a complete map of all proton–proton J-connectivities in the polypeptide chain, i.e. a map of through-bond connectivities between hydrogen atoms that are normally separated by not more than 3 chemical bonds in the covalent structure.

Through-space ^{1}H–^{1}H connectivity maps were obtained with 2-dimensional nuclear Overhauser enhancement spectroscopy. NOESY spectra were recorded with a sequence of 3 non-selective 90° pulses (Jeener *et al.*, 1979; Anil Kumar *et al.*, 1980*a*):

$$(90° - t_1 - 90° - \tau_m - 90° - t_2)_n.$$

After frequency labelling of the various magnetization components during t_1, cross-relaxation leads to incoherent magnetization exchange during the mixing time τ_m. The signal is recorded immediately after the third pulse as a function of t_2. Otherwise, the recording of the data is analogous to the procedures used for the COSY spectra, and the final appearance of the 2 spectra is very similar. In the place of the J-cross peaks in COSY, the NOESY spectra contain NOE cross peaks, which manifest spatial proximity between individual hydrogen atoms. In Fig. 2, a NOESY spectrum is presented as a contour plot. While aesthetically a contour plot may be less appealing than the 3-dimensional view of the spectrum in Fig. 1, it is a much more useful presentation for spectrum analysis, and all further spectra in this and the following paper are shown in this form. To illustrate the

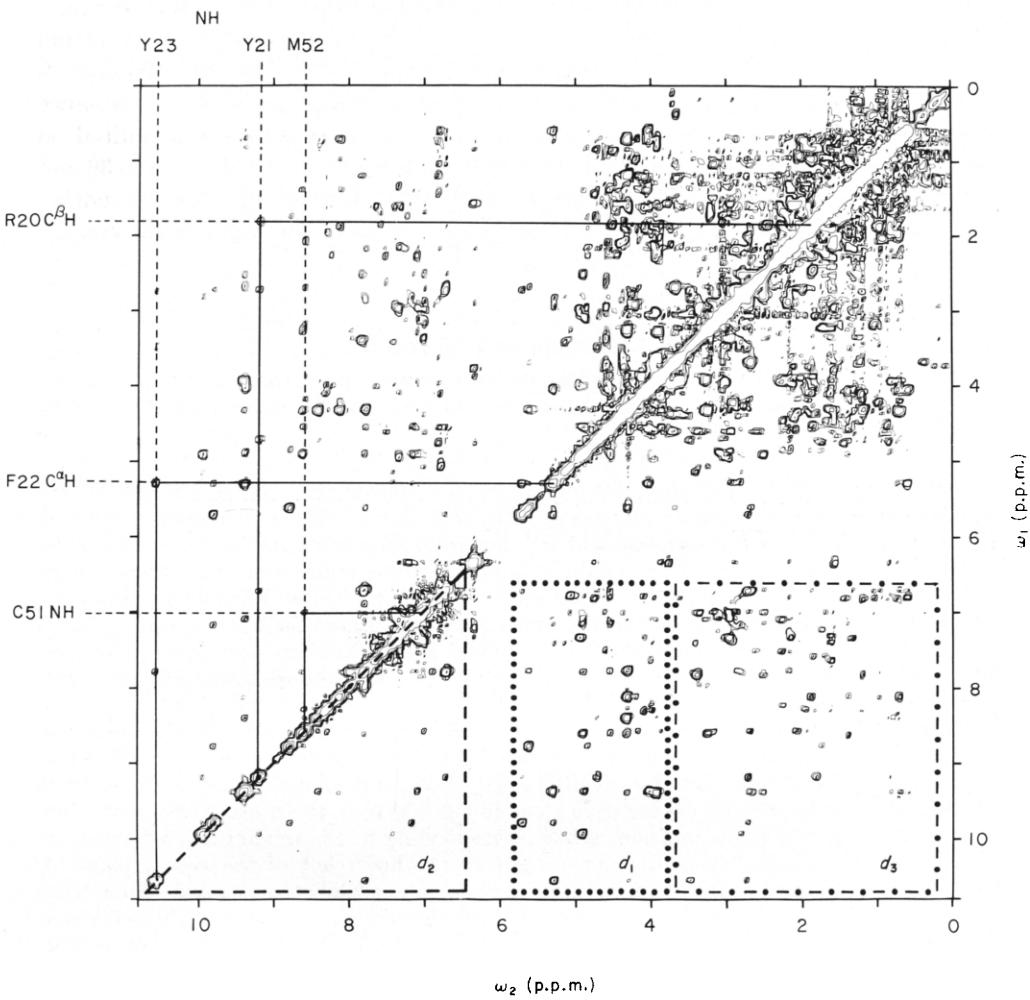

FIG. 2. Contour plot of a symmetrized, absolute value 500 MHz ^{1}H NOESY spectrum of a 0·02 M solution of BPTI in ^2H_2O, p^{2}H 4·6, $t = 36°C$. The digital resolution is 5·3 Hz/point. The spectrum was recorded in ~ 6 h, immediately after dissolving the protein in ^2H_2O, so that in addition to the non-labile protons the resonances of ~ 30 backbone amide protons are seen between 7 and 10·6 p.p.m. A 3-dimensional view of this spectrum would be closely similar to that of Fig. 1. The 2 frequency axes ω_1 and ω_2 are again calibrated with the chemical shifts, and peaks corresponding to the resonance positions in the normal, one-dimensional spectrum are on the diagonal from the upper right to the lower left corner. In the lower right triangle, 3 spectral regions of interest for sequential resonance assignments are outlined, i.e. the regions where NOE connectivities between different amide protons (– – –, d_2), between amide protons and C^{α} protons (· · ·, d_1) and between amide protons and C^{β} protons (–·–·–, d_3) are usually observed. In the upper left triangle, the analysis of such spectra is illustrated with 1 of each of these 3 types of connectivities. The continuous lines indicate the connectivities between cross peaks and diagonal peaks and the broken lines lead to the assignments of the connected resonances, which are indicated on the periphery of the Figure.

interpretation of such spectra, the connectivities for selected cross peaks have been indicated, and the connected protons identified in the upper left triangle of the spectrum in Fig. 2. In the lower right triangle, those spectral regions are outlined where the NOE cross peaks needed for sequential resonance assignments (Billeter *et al.*, 1982) are usually observed, i.e. those between different amide protons (d_2), between amide and C^{α} protons (d_1), and between amide and C^{β} protons (d_3). Obviously, in the COSY spectrum the J-connectivities between NH_i and $C^{\alpha}H_i$ are usually manifested in the spectral region that corresponds to d_1 in Fig. 2.

In contrast to the J-connectivities in COSY, a NOESY experiment cannot, with a single instrument setting, provide complete information on all NOE connectivities in a protein. The intensities of the NOE cross peaks in NOESY spectra vary over a period of several hundred ms (Anil Kumar *et al.*, 1981) and, for each individual peak, the initial build-up rate is proportional to the reciprocal of the sixth power of the distance between the 2 connected groups of protons (Solomon, 1955; Noggle & Schirmer, 1971). When long mixing times are used, this quantitative relation between internuclear distance and NOE intensity may be masked by spin diffusion and other relaxation effects, which jeopardize quantitative analyses of the data (Kalk & Berendsen, 1976; Gordon & Wüthrich, 1978; Wagner & Wüthrich, 1979*b*). For sequential resonance assignments, however, we need at most semi-quantitative distance information, i.e. the mixing time should be chosen just long enough that NOEs manifesting distances of $\lesssim 3{\cdot}0$ Å between different protons of the polypeptide backbone (Billeter *et al.*, 1982) are manifested with a workable signal to noise ratio. Detailed studies of the NOE buildup rates in BPTI (Dubs *et al.*, 1979; Wagner & Wüthrich, 1979*b*; Anil Kumar *et al.*, 1981) showed that, at frequencies between 360 and 500 MHz, a mixing time of 100 ms, which is the value used in all NOESY experiments reported in this paper, is adequate for this purpose.

Two-dimensional ^{1}H n.m.r. spectra at 500 MHz were recorded on a Bruker WM500 spectrometer. The spectra in Figs 1 to 3 and 5 to 8 were obtained from 512 measurements with t_1 values from 0 to 48 ms, the spectrum in Fig. 9 from 256 measurements with t_1 values from 0 to 28 ms. Quadrature detection was used for detection of the individual free induction decays, with the carrier frequency at the low field end of the spectrum. To eliminate experimental artifacts, groups of 16 recordings with different phases were added for each value of t_1 (Nagayama *et al.*, 1979,1980). For measurements in H_2O, the solvent resonance was suppressed by selective, continuous irradiation at all times except during data acquisition (t_2) (Anil Kumar *et al.*, 1980*b*). Usually, 2048 data points were used to store the data for each value of t_1 for all spectra, except that of Fig. 9, where 1024 data points were used. Before Fourier transformation, the time domain data matrix was multiplied in the t_1 direction with a phase-shifted sine bell, $\sin(\pi(t+t_0)/t_s)$, and in the t_2 direction with a phase-shifted sine-squared bell, $\sin^2(\pi(t+t_0)/t_s)$. The length of the window functions, t_s, was adjusted for the bells to reach zero at the last experimental data point in the t_1 or t_2 direction, respectively. The phase shifts, t_0/t_s, were $\frac{1}{32}$ and $\frac{1}{64}$ in the t_1 and t_2 directions, respectively. Furthermore, to end up with a 1024×1024 point data matrix in the frequency domain, which corresponds to a digital resolution of 5·3 Hz/point in Figs 1 to 3 and 5 to 8 and 4·3 Hz/point in Fig. 9, the time domain matrix was expanded to 2048 points in t_1 and 4096 points in t_2 by "zero-filling". The spectra in Figs 1 and 2 were further improved by symmetrization (Baumann *et al.*, 1981). All spectra are shown in the absolute value presentation.

Basic pancreatic trypsin inhibitor (Trasylol®, Bayer Leverkusen) was obtained from the Farbenfabriken Bayer AG. Four different samples were used for the present studies. All 4 contained 0·02 M-BPTI and the pH was adjusted by addition of minute amounts of HCl and NaOH, whereby in the ^2H_2O solutions the pH meter readings were used without correction for isotope effects (Kalinichenko, 1976; Bundi & Wüthrich, 1979*a*). The solvent for the first sample was a mixture of 90% H_2O and 10% ^2H_2O (pH 4·6), so that all the backbone amide proton resonances were present in the spectrum. The second and the third sample used ^2H_2O as a solvent, with p^{2}H 4·6 and 3·5, respectively, so that at low temperatures ~ 30 slowly

exchanging amide protons could be observed (Wüthrich & Wagner, 1979). In the fourth sample, all the labile protons had been replaced by ^2H by heating a ^2H_2O solution of BPTI (p^{2}H 4·6), to 85°C for 10 min. In the ^2H_2O solutions, the concentration of residual solvent protons was minimized by repeated lyophilization from ^2H_2O. Chemical shifts are quoted relative to internal sodium 3-trimethylsilyl-[2,2,3,3-$^2H_4$]propionate.

3. Results and Discussion

(a) *General considerations on the experimental realization of sequential resonance assignments*

The fundamental elements of sequential resonance assignments in polypeptide chains are given on the one hand by the experience gained in the first investigations of this type (Dubs *et al.*, 1979; Wagner *et al.*, 1981) and the results of the theoretical study in the preceding paper (Billeter *et al.*, 1982), and on the other hand by the potentialities of the two-dimensional n.m.r. experiments COSY and NOESY described in Materials and Methods. Hence, from COSY one determines the J-connectivities between the amide, C^α and C^β protons of the individual residues. From NOESY spectra recorded with suitable mixing times, one then obtains connectivities between neighbouring residues. Depending on whether this connectivity is based on the observation that one or two of the distances d_1 (from NH_{i+1} to $C^\alpha H_i$), d_2 (from NH_{i+1} to either NH_{i+2} or NH_i) or d_3 (from NH_{i+1} to $C^\beta H_i$) are $\lesssim 3{\cdot}0$ Å, its reliability varies from $\sim 70\%$ to 99% (Billeter *et al.*, 1982). In addition to these fundamental considerations, the following are helpful practical aspects.

(1) In the $NH_i - C^\alpha H_i$ region of the COSY spectrum of a protein in H_2O (Fig. 3), each residue gives rise to one peak, with the exception of glycine, which may give one or two peaks, proline, which is not represented in this region, and possibly the residues in the N-terminal dipeptide segment, where the NH exchange with the solvent may be too fast for the cross peaks to be observed (Bundi & Wüthrich, 1979*b*). The COSY spectrum thus provides a first "fingerprint" of the protein.

(2) As far as possible, the complete spin systems of the individual amino acid residues (Wüthrich, 1976) should be identified at the outset of the investigation. All the COSY peaks in the NH_i–$C^\alpha H_i$ region that belong to an identified spin system can then be assigned either to a specific amino acid type or to a small selection of amino acid types (but of course not to the sequence positions as in Fig. 3, where the final result of the present paper is indicated). This can greatly aid the subsequent sequential resonance assignments. Firstly, inspection of amino acid sequences (Dayhoff, 1972) shows that, once the sequential assignments in the early stages of the analysis extend over two to four identified amino acid types, one can locate the assigned peptide segment in the sequence. Secondly, for all subsequent sequential assignments leading to COSY peaks of specific amino acid types, the amino acid sequence provides an immediate check on the sequential assignment. This is particularly helpful for resolving ambiguities in the sequential assignments that may arise when two or several residues have identical NH and/or $C^\alpha H$ chemical shifts. Thirdly, when the spin system of the amino acid residues is known and a sequential connectivity *via* either d_1, d_2 or d_3 has been established, the locations of

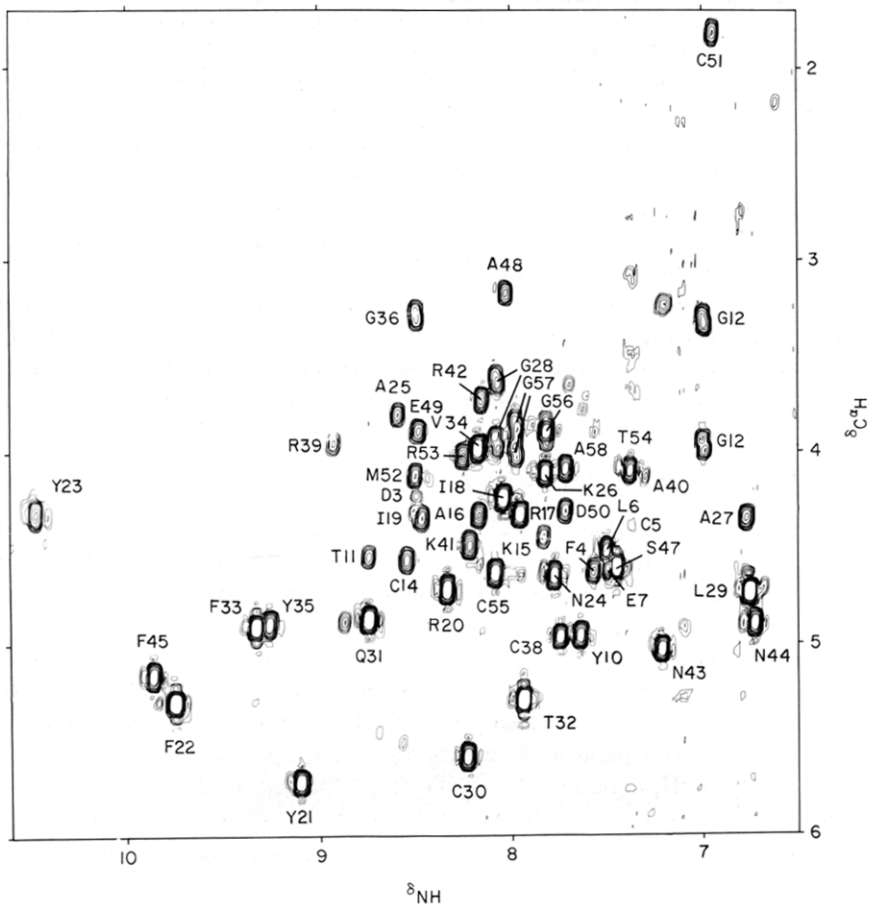

FIG. 3. Spectral region (1·7 to 6·0 p.p.m.) × (6·6 to 10·6 p.p.m.) of a 500 MHz ^{1}H COSY spectrum of BPTI in H_2O recorded at 68°C in the sample described in the legend to Fig. 1. The spectrum was recorded in ~ 17 h, the digital resolution is 5·3 Hz/point. The letters and numbers indicate the resonance assignments of the $C^{\alpha}H$–NH J-connectivities for all the residues in the amino acid sequence of BPTI, except Arg1, where the N-terminal amino protons exchange probably too rapidly to be observed, the 4 proline residues, and Gly37. The cross peak of Lys46 is not visible in this spectrum, since at 68°C it coincides in the ω_1 direction with the water signal and is therefore bleached out by the solvent irradiation (see Table 1).

the NOESY peaks manifesting the other two connectivities is known *a priori*, and hence these can be studied more efficiently.

(3) In many proteins, a considerable number of interior amide protons exchange slowly with the solvent. It may be advantageous to start the sequential assignments in the simplified spectra obtained when such proteins are dissolved in ^2H_2O (Wüthrich, 1976). When the interior amide protons are pre-exchanged with ^2H, a simplified spectrum may also be obtained in H_2O solution.

(4) In the advanced stages of the sequential assignments, the protein fingerprint in the NH_i–$C^{\alpha}H_i$ region of the COSY spectrum provides a quite natural check for

each successive assignment, in that each peak must be assigned once and only once in the entire analysis (Fig. 3).

(5) As soon as all but one residue of a specific amino acid type are assigned, identification of the side-chain spin system is sufficient to locate the remaining residue in the amino acid sequence. Quite sizeable peptide segments may thus be assigned in the final stages of the experiment. However, with regard to the determination of the secondary structure, it is nevertheless advantageous to further investigate the sequential connectivities for these residues (W. Braun, M. Billeter, & K. Wüthrich, unpublished results).

(6) The complex spin systems of the long amino acid side-chains are usually difficult to identify. However, once the chemical shifts of the C^{α} and C^{β} protons are known from the sequential assignments, one has often a much better chance to extend the assignments to the peripheral groups of hydrogen atoms.

(b) *Strategy used to assign the ^1H n.m.r. spectrum of BPTI*

A survey of the experimental evidence accumulated to assign the ^1H n.m.r. spectrum of BPTI is presented in Figure 4, and the chemical shifts of the assigned resonances are listed in Table 1. Initial sequential assignments were obtained in the simplified ^1H n.m.r. spectra recorded in freshly prepared ^2H_2O solutions of the protein (Dubs *et al.*, 1979). These were then extended by studies in H_2O, as indicated by the stars in Figure 4 (Wagner *et al.*, 1981). All these earlier assignments were based on single NOE connectivities between the individual residues, i.e. d_1 for the peptide segments 16 to 25, 29 to 36 and 43 to 45, and

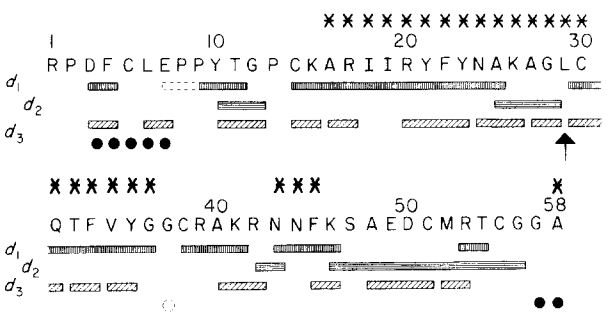

FIG. 4. Amino acid sequence of BPTI and survey of the experimental evidence by which the individual resonance assignments were obtained. ([▥]) Sequential assignments *via* d_1 (NOE from NH_{i+1} to $C^{\alpha}H_i$); ([▤]) sequential assignments *via* d_2 (NOE from NH_{i+1} to NH_i); ([▨]) sequential assignments *via* d_3 (NOE from NH_{i+1} to $C^{\beta}H_i$); ([┅]) sequential assignments *via* NOEs from Pro $C^{\delta}H_{i+1}$ to $C^{\alpha}H_i$. (○, ●) The individual assignment relied primarily on the identification of the complete spin system of the amino acid residue without or with the amide proton, respectively. Once all but one residue of a given type has been assigned, this information is obviously sufficient for the individual assignment in the amino acid sequence even when neither of the connectivities d_1, d_2 or d_3 could be established. The arrow indicates a location where all the resonances were assigned, but the connectivity between 2 neighbouring residues was not established. Stars (*) above the sequence identify the residues for which complete resonance assignments had been obtained in previous work (Dubs *et al.*, 1979; De Marco *et al.*, 1977; Anil Kumar *et al.*, 1980*b*; Wagner *et al.*, 1981).

TABLE 1

Chemical shifts, δ†, of the assigned ^{1}H n.m.r. lines of BPTI. pH 4·6, t = 68°C

Amino acid residue	δ (±0·01 p.p.m.)†‡			
	NH	$C^{\alpha}H$	$C^{\beta}H$	Others
Arg1				
Pro2				
Asp3	8·49	4·23	2·79, 2·79	
Phe4	7·57	4·63	2·99, 3·34	$C^{\delta}H_2$ 7·01
				$C^{\epsilon}H_2$ 7·40
				$C^{\zeta}H$ 7·06
Cys5	7·37	4·39	2·75, 2·91	
Leu6	7·50	4·52	1·88, 1·88	$C^{\gamma}H$ 1·71
				$C^{\delta}H_3$ 0·88, 0·98
Glu7	7·50	4·61	2·18, 2·27	$C^{\gamma}H_2$ 2·58, 2·58
Pro8		4·67	1·88, 2·45	$C^{\gamma}H_2$ 2·12
				$C^{\delta}H_2$ 3·70, 3·98
Pro9		3·77	0·14, 0·27	$C^{\gamma}H_2$ 0·19, 1·30
				$C^{\delta}H_2$ 2·97, 3·18
Tyr10	7·64	4·96	2·95, 2·95	$C^{\delta}H_2$ 7·34
				$C^{\epsilon}H_2$ 7·10
Thr11	8·74	4·55	4·07	$C^{\gamma}H_3$ 1·40
Gly12	7·00	3·32, 3·97		
Pro13				
Cys14	8·54	4·56	2·81, 3·48	
Lys15	7·83	4·45	1·59, 2·08	$C^{\gamma}H_2$ 1·31, 1·41
Ala16	8·17	4·33	1·18	
Arg17	7·95	4·33	1·63, 1·63	
Ile18	8·04	4·24	1·90	$C^{\gamma}H_2$ 1·07
				$C^{\gamma}H_3$ 0·97
				$C^{\delta}H_3$ 0·73
Ile19	8·46	4·35	1·96	$C^{\gamma}H_2$ 1·46
				$C^{\gamma}H_3$ 0·74
				$C^{\delta}H_3$ 0·73
Arg20	8·33	4·72	0·86, 1·83	$C^{\gamma}H_2$ 1·37, 1·72
				$C^{\delta}H_2$ 3·08, 3·48
				$N^{\delta}H$ 7·37
Tyr21	9·10	5·71	2·72, 2·72	$C^{\delta}H_2$ 6·74
				$C^{\epsilon}H_2$ 6·79
Phe22	9·74	5·30	2·85, 2·96	$C^{\delta}H_2$ 7·16, 7·27
				$C^{\epsilon}H_2$ 6·98, 7·07
				$C^{\zeta}H$ 7·31
Tyr23	10·46	4·32	2·74, 3·49	$C^{\delta}H_2$ 7·19
				$C^{\epsilon}H_2$ 6·35
Asn24	7·78	4·65	2·18, 2·86	$N^{\delta}H_2$ 6·96, 7·79
Ala25	8·59	3·81	1·58	
Lys26	7·82	4·11	1·89	
Ala27	6·77	4·35	1·20	
Gly28	8·07	3·64, 3·95	—	
Leu29	6·76	4·73	1·45, 1·69	$C^{\gamma}H$ 1·44
				$C^{\delta}H_3$ 0·78, 0·87
Cys30	8·23	5·58	2·71, 3·63	
Gln31	8·74	4·87	1·77, 2·16	$C^{\gamma}H_2$ 1·83, 2·02
				$N^{\epsilon}H_2$ 7·22, 7·30
Thr32	7·94	5·24	4·04	$C^{\gamma}H_3$ 0·62
Phe33	9·32	4·91	2·98, 3·13	$C^{\delta}H_2$ 7·13
				$C^{\epsilon}H_2$ 7·20
				$C^{\zeta}H$ 7·33

TABLE 1 (*continued*)

Amino acid residue	δ(±0·01 p.p.m.)†‡			
	NH	$C^{\alpha}H$	$C^{\beta}H$	Others
Val34	8·17	3·98	1·96	$C^{\gamma}H_3$ 0·73, 0·83
Tyr35	9·26	4·90	2·52, 2·64	$C^{\delta}H_2$ (6·77, 7·76)§
				$C^{\epsilon}H_2$ 6·83
Gly36	8·49	3·28, 4·33		
Gly37	n.o.	2·92, 4·24		
Cys38	7·74	4·97	3·15, 3·80	
Arg39	8·92	3·95	2·26, 2·26	
Ala40	7·30	4·13	1·23	
Lys41	8·22	4·49	1·67, 2·26	$C^{\gamma}H_2$ 1·32, 1·49
Arg42	8·15	3·73	0·53, 1·18	$C^{\gamma}H_2$ 1·22, 1·48
				$C^{\delta}H_2$ 2·76, 2·86
				$N^{\epsilon}H$ 6·80
Asn43	7·22	5·03	3·28, 3·34	$N^{\delta}H_2$ 7·77, 7·97
Asn44	6·73	4·90	2·54, 2·80	
Phe45	9·85	5·16	2·80, 3·41	$C^{\delta}H_2$ 7·39
				$C^{\epsilon}H_2$ 7·87
				$C^{\zeta}H$ 7·62
Lys46	9·71	4·37	0·95, 2·01	
Ser47	7·46	4·60	3·90, 4·16	
Ala48	8·03	3·17	1·05	
Glu49	8·48	3·89	1·77, 2·02	$C^{\gamma}H_2$ 2·23, 2·36
Asp50	7·72	4·31	2·73, 2·73	
Cys51	6·95	1·81	2·90, 3·15	
Met52	8·50	4·12	2·00, 2·06	$C^{\gamma}H_2$ 2·70, 2·70
				$C^{\epsilon}H_3$ 2·16
Arg53	8·25	4·02	1·61	
Thr54	7·38	4·10	3·95	$C^{\gamma}H_3$ 1·59
Cys55	8·09	4·63	1·98, 2·23	
Gly56	7·82	3·90, 3·90		
Gly57	7·98	3·87, 4·01		
Ala58	7·72	4·09	1·32	

† The chemical shifts, δ, are relative to internal sodium 3-trimethylsilyl-[2,2,3,3-$^2H_4$]propionate.

‡ Where no numbers are given in the columns for NH, $C^{\alpha}H$ and $C^{\beta}H$ and where more peripheral side-chain hydrogen atoms are not listed in the last column, no individual resonance assignments were obtained (see the text).

§ At 68°C, the C^{δ} proton resonances of Tyr35 are broadened by the ring flipping (Wagner *et al.*, 1976). Therefore, the chemical shifts observed at 36°C are listed. n.o., not observed.

d_2 for the segment 25 to 29. To further improve the reliability (Billeter *et al.*, 1982) of these earlier results, a second connectivity was now established in most cases (Fig. 4). The sequential assignments were then extended to the other regions of the polypeptide chain. As far as possible, we tried to add onto the previously assigned peptide segments, so that the amino acid sequence could be consulted continuously to check on the sequential assignments. Figure 4 shows that, to a considerable extent, the new assignments relied on two connectivities, mainly either on d_1 and d_3, or on d_2 and d_3. In Figures 5 to 8, each step of the new sequential assignments is documented by one connectivity, usually the one that was established first.

In Figure 4, an important contribution to the spectral assignments is explicitly shown only for a few residues, i.e. the identification of the amino acid side-chain spin systems. For the technical aspects, we refer to the descriptions by Nagayama & Wüthrich (1981) of the spin system identifications in BPTI using spin echo correlated spectroscopy (SECSY) and by Wider *et al.* (1982, following paper) of the spin system identifications in glucagon using COSY. In BPTI, 41 side-chains were identified at the outset of the study. With regard to using the amino acid sequence (Fig. 4) as a check of the sequential assignments in BPTI, the following groups of different spin systems were then available: five Gly, five Ala, Ala58, three Thr, Val34, two Asp, two Glu, Ser47, 17 ABX and A_2X spin systems, two five-spin systems (Met and Gln), two Ile, and 12 "long side-chains" (Leu, Lys, Arg) (Nagayama & Wüthrich, 1981). Since many of these spin systems were already assigned to specific locations in the β-sheet region (starred residues in Fig. 4), the remaining spin systems provided quite stringent criteria to check on the new sequential assignments.

In the final stages of the spectrum analysis, a sizeable proportion of the resonances in the side-chains of leucine, proline, lysine and arginine could be assigned, starting from the sequentially assigned $C^\alpha H$ and $C^\beta H$ lines. Furthermore, as documented in Figure 9, connectivities with the peripheral protons in the aromatic side-chains of asparagine and glutamine were established *via* NOE measurements (Billeter *et al.*, 1982).

(c) *Sequential resonance assignments in the C-terminal α-helix region*

The first step in the assignments from the previously identified tripeptide, segment 43 to 45, to the C terminus was *via* a d_1 connectivity between Phe45 $C^\alpha H$ and Lys46 NH (Fig. 5). As previously shown (Wagner *et al.*, 1981), d_1 connectivities are readily documented in "combined COSY–NOESY connectivity diagrams". These diagrams make use of the fact that the information in a COSY or NOESY spectrum is contained redundantly in the two triangles separated by the diagonal peaks (Figs 1 and 2). When the upper left triangle of NOESY and the lower right triangle of COSY are added, the combined plot manifests the through-space NOE connectivities between NH_{i+1} and $C^\alpha H_i$, as well as the through-bond J-connectivities between $C^\alpha H_i$ and NH_i. A record of sequential assignments *via* d_1 then consists of a spiral-like connectivity pattern. In Figure 5, where only those regions are displayed that contain the $C^\alpha H$–NH cross peaks (Fig. 2), a horizontal line leads from the position of the Lys46 $C^\alpha H$–NH COSY peak to the virtual diagonal position of the amide proton resonance. There is a single NOESY cross peak with the Lys46 NH chemical shift, which is therefore assigned to $C^\alpha H$ of Phe45 (in Fig. 5, a vertical line connects this peak with the diagonal position of Lys46 NH). Continuing on, a horizontal line leads to the virtual diagonal position of $C^\alpha H$ of Phe45, from where a vertical line connects with the previously assigned $C^\alpha H$–NH COSY peak of Phe45.

The following assignments were *via* d_2 connectivities between amide protons of neighbouring residues, as documented in the low-field region of the NOESY

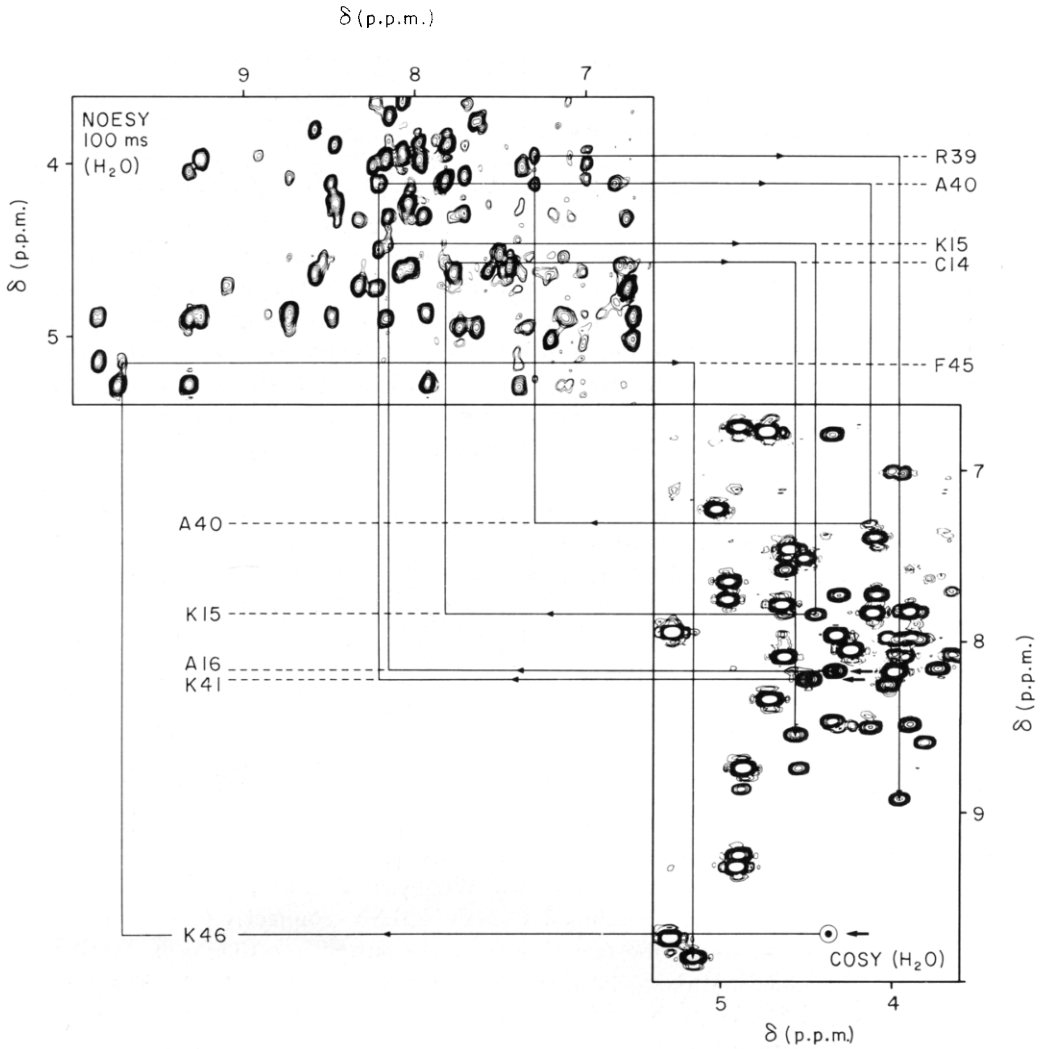

FIG. 5. Combined COSY–NOESY connectivity diagram for sequential resonance assignments *via* NOEs between NH and the $C^{\alpha}H$ of the preceding residue (d_1) (Wagner *et al.*, 1981). In the upper left the region (3·6 to 5·4 p.p.m.) × (6·6 to 10·0 p.p.m.) from the NOESY spectrum of Fig. 6 is shown. In the lower right, the corresponding region from the COSY spectrum in Fig. 3 is shown, which was recorded from the same sample and under identical conditions. The straight lines and arrows indicate the sequential resonance assignments obtained for the segments 46 to 45, 41 to 39 and 16 to 14. Starting points are indicated by the arrows in the COSY spectrum. At 68°C, the NH–$C^{\alpha}H$ cross peak for Lys46 in the COSY spectrum was bleached out by the irradiation of the solvent, since the $C^{\alpha}H$ resonance coincides with that of H_2O. It was, however, observed at different temperatures.

spectrum in Figure 6. As was discussed in detail in the preceding paper (Billeter *et al.*, 1982), d_2 connectivities are symmetrical with respect to the direction of the polypeptide chain, and hence an NH–NH NOE connectivity may equally well be with either of the two neighbouring residues in the sequence. However, when the NH chemical shift of one of these residue is known independently, the direction of

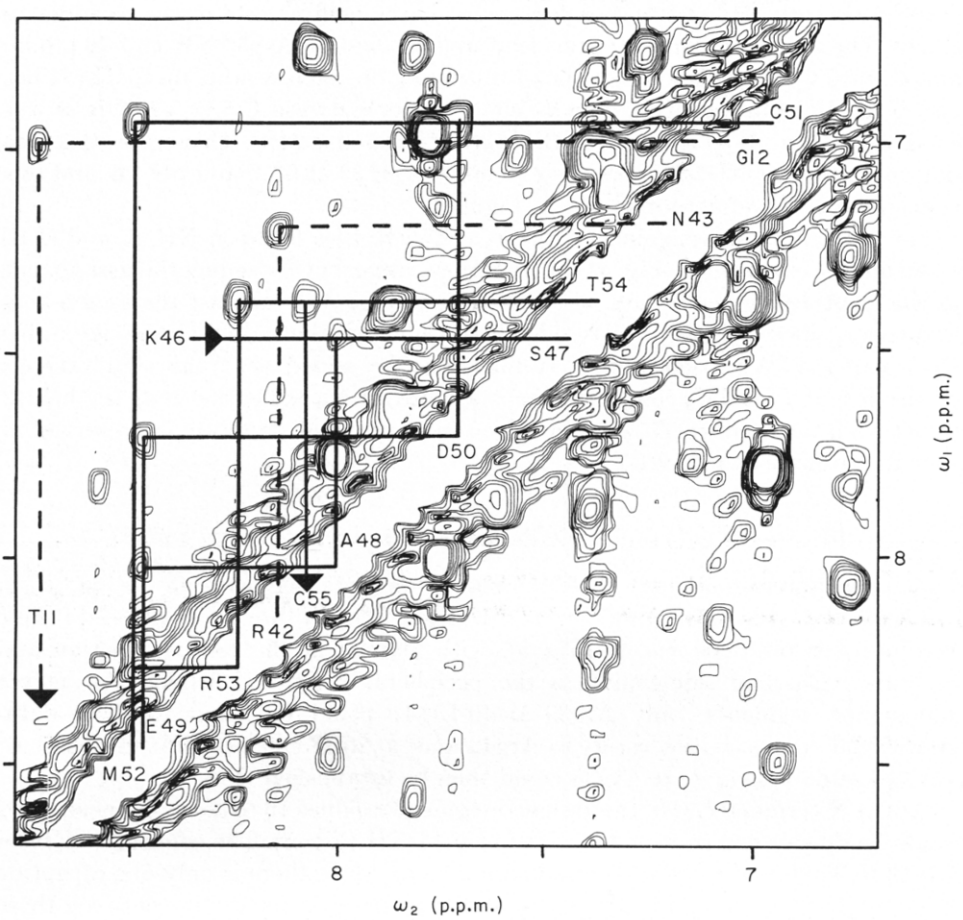

FIG. 6. Contour plot of the spectral region from 6·6 to 8·7 p.p.m. of a NOESY spectrum recorded at 68°C from the same sample and under identical conditions as the COSY spectrum of Fig. 3. This spectral region contains the diagonal peaks of most of the backbone amide protons and the cross peaks manifest NOEs between different amide protons. The solid lines indicate the sequential assignments for the polypeptide segment 46 to 55, which were obtained from NH–NH NOEs (d_2). The arrows indicate the start and the end of this sequence. The NOE cross peak between the amide proton resonances of Lys46 and Ser47 is not shown, since at (ω_1 = 7·47 p.p.m., ω_2 = 9·71 p.p.m.) it is outside of this spectral region. Connectivities between the amide protons of Thr11 and Gly12, and of Arg42 and Asn43 are indicated by broken lines.

the sequential connectivity is determined. Here, the first connectivity to be established was from Lys46 to Ser47. Since Phe45 NH was known (Fig. 5), the only NH–NH NOESY peak involving Lys46 had to be with Ser47. Because of the symmetry of d_2-connectivities, a second cross peak linking NH of Ser47 with NH of residue Ala48 might be present, depending on the local conformation (Billeter *et al.*, 1982). Since the amide proton of Ala48 might be to higher or lower field, this second cross peak could be either vertically above or horizontally to the left of the diagonal peak of Ser47 NH. Figure 5 shows that it is on the left, at ω_2 = 8·03 p.p.m. The second

cross peak with NH of Ala48 is further to lower field at 8·48 p.p.m., leading to Glu49. The next two connectivities lead upfield, first to Asp50 NH at 7·72 p.p.m. and then to Cys51 NH at 6·95 p.p.m. Continuing on, each residue up to Thr54 has two NH–NH connectivities. The d_2 connectivity between Cys55 and Gly56 was established in a ^2H_2O solution of BPTI at p^{2}H 3·5 and 24°C. This cross peak was not present in the NOESY spectrum recorded in H_2O at 68°C and pH 4·6, and this connection is therefore not shown in Figure 6.

For most of these assignments, the d_3 connectivities between NH_{i+1} and $C^{\beta}H_i$ could also be established (Fig. 4). Furthermore, almost every sequential assignment in this peptide segment could be checked unambiguously against the amino acid sequence, since all but two side-chain spin systems had been identified (Nagayama & Wüthrich, 1981). It may also be added that the simultaneous occurrence of d_2 and d_3 connectivities is a quite strong indication that the helical structure from residues 47 to 55 observed in the crystal structure is preserved in solution (Billeter *et al.*, 1982).

(d) *Sequential assignments in the central and N-terminal regions*

At the N-terminal end of the assigned peptide segment 43 to 56, a d_2 connectivity leads to the amide proton of Arg42 (Fig. 6). Next, a sequence of three residues was obtained *via* d_1 (Fig. 5), with alanine in the central position and residues with long side-chains in the peripheral positions. Among the as yet unassigned segments, only Arg39-Ala40-Lys41 could be fitted to these data. Additional connectivities *via* d_3 to Arg42 and, at different temperature (56°C) or pH (3·5 at 68°C), *via* d_1 to Cys38 could then be established (Fig. 4).

At the N-terminal end of the assigned segment residues 16 to 36, d_1 connectivities could be established from Ala16 $C^{\alpha}H$ to Cys14 NH (Fig. 5). The connectivity from Gly12 to Thr11 *via* d_2 (Fig. 6) was unambiguous, since there is only one dipeptide segment Thr-Gly in BPTI (Fig. 4). In addition, the d_3 connectivity between these two residues could also be established and, as described in Figure 7, two successive d_1 connectivities provided the assignments for Tyr10 and for Pro9 $C^{\alpha}H$. The assignment of the proline C^{α} proton is consistent with the observation that there is no NH–$C^{\alpha}H$ J-peak at 3·77 p.p.m. in the COSY spectrum of Figure 3.

The spin system of Pro9 could now be completely characterized in the COSY spectrum (Fig. 8). It is characterized by extreme high-field positions of the two C^{β} protons and one C^{γ} proton (Table 1). On the basis of NOEs with Pro9 $C^{\delta}H$ (Billeter *et al.*, 1982), the C^{α} proton of Pro8 was assigned and subsequently linked to the C^{β}, C^{γ} and C^{δ} protons *via* J-connectivities in the COSY spectrum (Fig. 8). The assignment of Pro8 $C^{\alpha}H$ coincided again with the observation that there is no NH–$C^{\alpha}H$ J-peak at 4·67 p.p.m. in the COSY spectrum of Figure 3. Finally, NOE connectivities with Pro8 $C^{\delta}H_2$ led to $C^{\alpha}H$ of Glu7, which was also assigned independently from the identification of the side-chain spin system.

At this stage, only the residues 1 to 6, 13, 37 and 57 were not yet assigned. Each residue type in the sequence 3 to 6 thus occurred only once among the unassigned residues (Fig. 4) and was therefore unambiguously assigned from the identification of the side-chain spin system. In addition, sequential connectivities could be

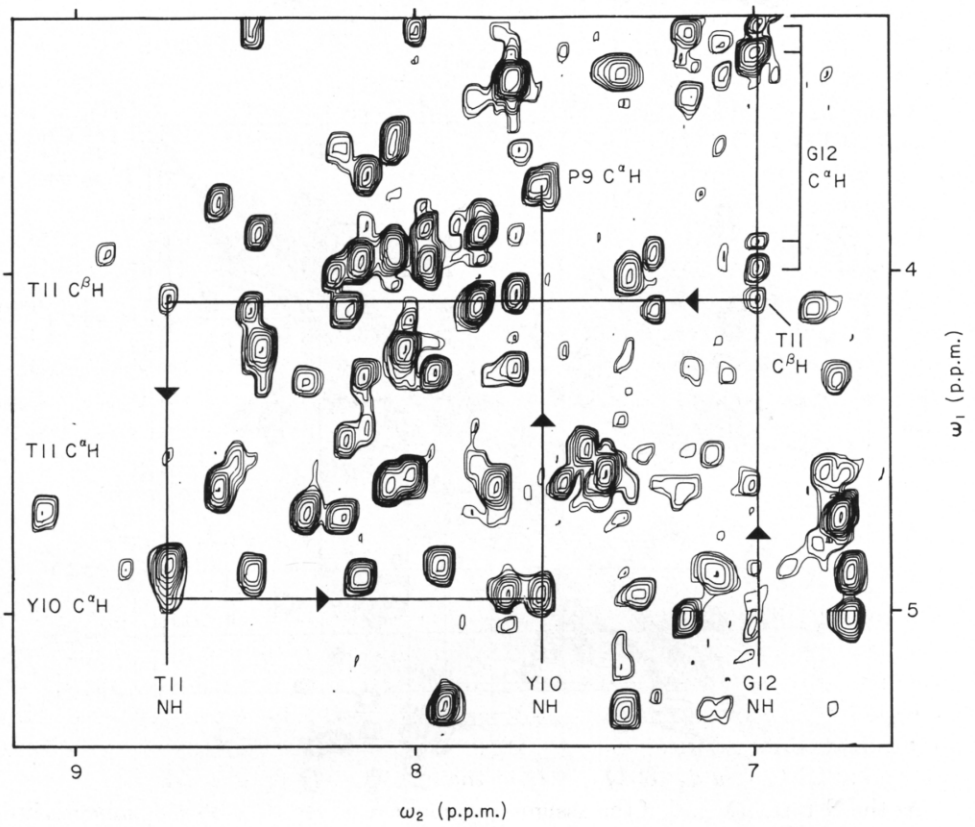

FIG. 7. Contour plot of the spectral region (3·2 to 5·4 p.p.m.) × (6·6 to 9·2 p.p.m.) of the same NOESY spectrum as in Fig. 6. The continuous lines indicate the sequential resonance assignments for the polypeptide segment 9 to 12, which were obtained from NOEs between the amide proton of Gly12 and the C^{β} proton of Thr11 (d_3), the amide proton of Thr11 and the C^{α} proton of Tyr10 (d_1), and the amide proton of Tyr10 and the C^{α} proton of Pro9 (d_1). The arrows indicate the direction of the sequence of assignments from residues 12 to 9.

established between Asp3 and Phe4 *via* d_1 and d_3, and between Leu6 and Glu7 *via* d_3. The $C^{\alpha}H_2$ resonances of Gly12 and Gly37 were previously assigned as a group from comparison of native BPTI with a chemical modification of the protein, where the disulfide bond 14–38 had been reduced (Nagayama & Wüthrich, 1981). Since Gly12 was identified (Figs 6 and 7), there remained only one AX spin system for $C^{\alpha}H_2$ of Gly37 (Table 1). The COSY cross peak with the amide proton of Gly37 was not observed, however, and no NOE connectivity with either Gly36 or Cys38 could be established. The C-terminal alanine was identified previously from the pH titration shift (De Marco *et al.*, 1977). The assignment of Gly57 relied on the identification of the spin system (Nagayama & Wüthrich, 1981), which was at this point the only glycine spin system that had not been assigned individually.

Returning at this point to the COSY spectrum of Figure 3, we find that with the assignments outlined in Figure 4 the $C^{\alpha}H$–NH cross peaks of 52

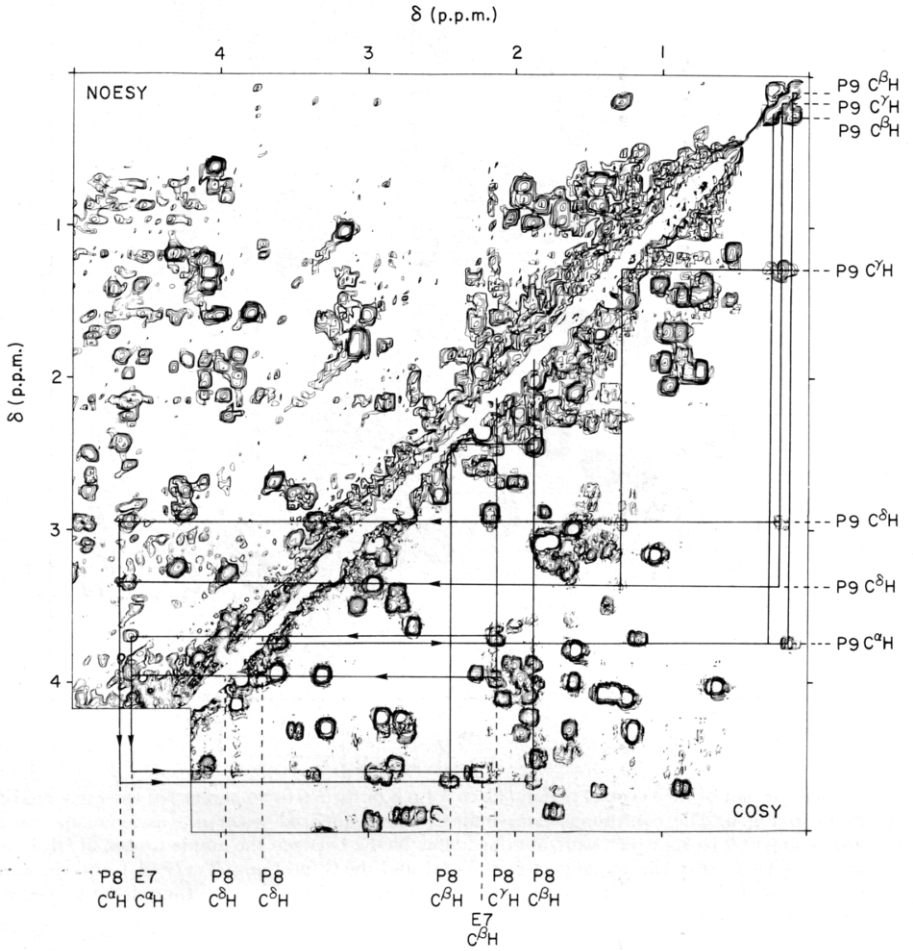

FIG. 8. Resonance assignments for the peptide segment Glu7-Pro8-Pro9 in BPTI. To document these data, the region (0·0 to 4·2 p.p.m.) × (0·0 to 5·0 p.p.m.) from the NOESY spectrum of BPTI in H_2O solution at 68°C (same spectrum as in Fig. 6) in the upper left triangle was combined with the corresponding region from a COSY spectrum (same as in Fig. 3) recorded from the same sample under identical conditions. Connectivities between peaks within COSY are indicated by continuous lines, connectivities between COSY and NOESY peaks by continuous lines with arrows. Starting from the previously assigned C^{α} proton (Fig. 7), the J-connectivities between the individual protons of Pro9 are indicated in the COSY spectrum, and the peaks identified on the right-hand margin. At the chemical shifts of each of the C^{δ} protons of Pro9, a cross peak was observed in the NOESY spectrum, which was assigned to $C^{\alpha}H$ of Pro8 (Billeter *et al.*, 1982). A vertical line leads through these 2 NOESY cross peaks to the diagonal position for $C^{\alpha}H$ of Pro8. Back in the COSY spectrum, the J-connectivities within the spin system of Pro8 are indicated, and the peaks identified at the bottom of the Figure. Only 1 connectivity with $C^{\gamma}H_2$ was observed, possibly because the 2 protons have identical chemical shifts. At the chemical shifts of each of the C^{δ} protons of Pro8, a strong peak was observed in the NOESY spectrum and assigned to $C^{\alpha}H$ of Glu7. Also indicated in the COSY spectrum is the previously identified (Nagayama & Wüthrich, 1981) $C^{\alpha}H$–$C^{\beta}H$ connectivity of Glu7, which provides an independent, final check for the assignments in this Figure.

residues were identified. There are a number of as yet unassigned, relatively weak peaks in the spectral region shown in Figure 3. Four of these could be assigned to the J-couplings between the labile side-chain protons of Arg20 and Arg42 with the C^{δ} methylene protons (see Table 1).

(e) *Resonance assignments in the long amino acid side-chains*

Starting with the sequentially assigned C^{α} and C^{β} protons, several spin systems of long amino acid side-chains could be completely or in part assigned *via* J-connectivities in the COSY and SECSY spectra. New complete assignments include Leu6, Pro8, Pro9, Ile18, Ile19, Leu29, Arg20 and Arg42.

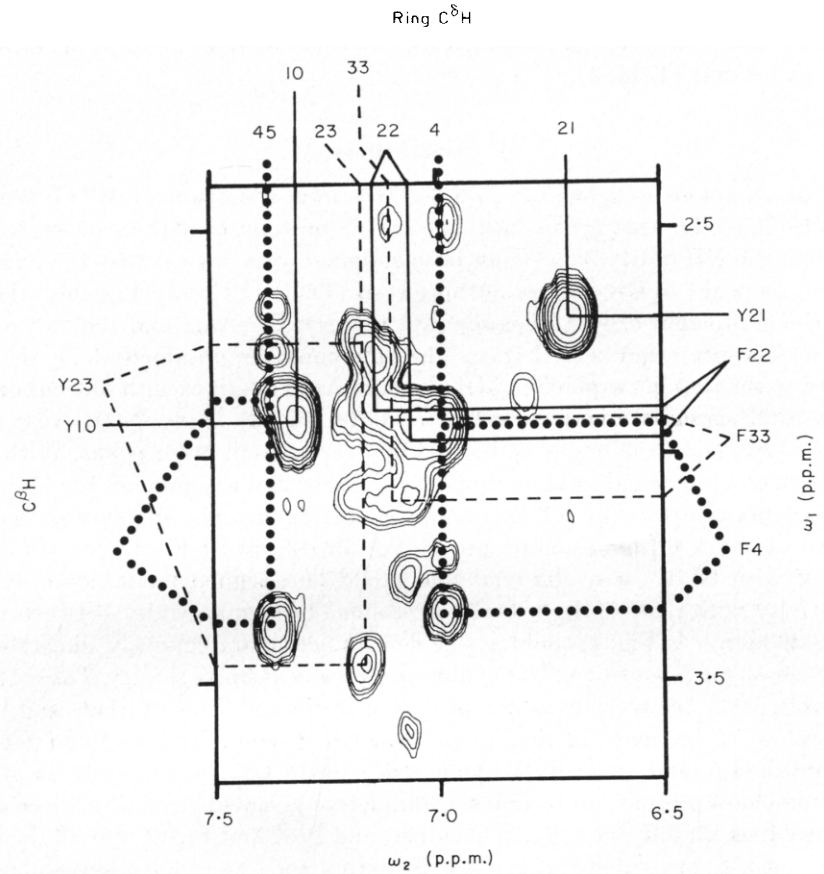

FIG. 9. Spectral region (2·4 to 3·7 p.p.m.) × (6·5 to 7·5 p.p.m.) of a 500 MHz ^{1}H NOESY spectrum of a 0·02 M solution of BPTI in ^2H_2O at 68°C, p^{2}H 4·6. All the labile protons had been replaced by ^{2}H. The spectrum was recorded in ~ 6 h, the digital resolution is 4·3 Hz/point. The spectrum shows NOE connectivities between the C^{β} protons and the aromatic C^{δ} protons of 7 of the 8 tyrosine and phenylalanine side-chains in BPTI. Tyr35 cannot be observed at this temperature, since the C^{δ}–H resonances are broadened due to low frequency ring flips (Wagner *et al.*, 1976). At lower temperatures, where sharp resonances are observed for the C^{δ} protons of Tyr35, the connectivity could be established readily.

Following the model calculations in the preceding paper (Billeter *et al.*, 1982), NOE connectivities were used to link the spin systems of the aromatic rings with the corresponding $C^{\alpha}H$–$C^{\beta}H_2$ fragments. The experimental evidence is presented in the NOESY spectrum of Figure 9. For the side-chains of Phe4, Tyr10, Tyr21, Tyr23, Tyr35 (not shown in Fig. 9, since it had to be measured at a different temperature (Wagner *et al.*, 1976)) and Phe45, unambiguous assignments were thus obtained. In all instances, these assignments coincide with those previously proposed on the basis of chemical modifications (Snyder *et al.*, 1975) or comparison of homologous proteins (Wagner *et al.*, 1978*a*,*b*). For Phe22 and Phe33, cross peaks in Figure 9 are compatible with the assignments obtained from comparison of homologous proteins, but the peaks are not sufficiently well-resolved to present clear-cut evidence for these assignments.

From similar studies of NOE peaks in the NOESY spectra recorded in H_2O, individual assignments were obtained for the side-chain amide protons of Asn24, Gln31 and Asn43 (Table 1).

4. Conclusions

Almost complete assignments of the ^1H n.m.r. spectrum of BPTI are now available (Table 1). Among the backbone and C^{β} protons, only those of Arg1, Pro2, Pro13 and the NH of Gly37 have not been assigned. It is unclear why the NH–$C^{\alpha}H$ COSY cross peaks of Gly37 were not observed (Table 1; Fig. 3). Possibly, the NH resonance is broadened by a dynamic rate process. For Arg1 and the two proline residues, it appears unlikely that assignments could be obtained along the lines followed in the present paper. The NH signal of Asp3 overlaps with four other lines and the $C^{\alpha}H$ signal overlaps with that of Ile18 (Fig. 3). Thus, NOE cross peaks between Asp3 and Pro2 might be hidden by overlap with other peaks. With Pro2 not assigned, one could mainly hope to achieve an assignment for Arg1 *via* complete identification of all the arginine side-chain spin systems or *via* pH titration of the N-terminal amino group. For Pro13, no NOE, either with NH of Cys14 or with Gly12, was observed that could be assigned unambiguously to a connectivity with $C^{\alpha}H$, $C^{\beta}H_2$ or $C^{\delta}H_2$ of proline. The connectivity between Gly28 and Leu29 (arrow in Fig. 4) could not be determined unambiguously, since the NH resonances of Ala27 and Leu29 have identical chemical shifts (Fig. 3; Table 1). The NOE cross peaks between the amide proton of Gly28 and those of Ala27 and Leu29 are therefore at the same position, so that the two d_2 connectivities could not both be established unambiguously (Wagner *et al.*, 1981). Of the spin systems of non-labile side-chain protons, all have been completely assigned except for those of the lysine residues, all but two arginine residues, and Pro2 and Pro13. For all the labile protons not listed in Table 1, it is most likely that they were not observed because of rapid exchange with the solvent (Wüthrich, 1976; Bundi & Wüthrich, 1979*a*,*b*).

The chemical shifts for all assigned resonances listed in Table 1 were measured at 68°C and pH 4·6. The Table is therefore more complete than previously published data sets, and also complementary, since the previous listings were for 36°C and pH 4·6 (Wüthrich & Wagner, 1979) and for 24°C and pH 4·6 (Nagayama & Wüthrich, 1981; Wagner *et al.*, 1981), respectively.

The principal project for further use of the presently described resonance assignments is the determination of the three-dimensional structure of BPTI in solution, as outlined in one of the preceding papers (Wüthrich *et al.*, 1982). There is already a lot of evidence that the core of the crystal structure is preserved in solution, both from the presently observed distribution of d_1, d_2 and d_3-connectivities along the amino acid sequence (Fig. 4) (Billeter *et al.*, 1982), as well as from earlier observations, e.g. NOEs between protons in the different strands of the β-sheet (Wagner *et al.*, 1981) or the coincidence with the present assignments of numerous previous assignments obtained with reference to the crystal structure (e.g. Wüthrich *et al.*, 1978; Perkins & Wüthrich, 1979). If further detailed checks confirm that there is close coincidence between extensive interior regions of the molecule in single crystals and in solution, BPTI will be a unique vehicle to further investigate the correlations between NOE intensities and proton–proton distances in proteins, which will be of crucial importance in view of further refined protein structure determinations by n.m.r. (Wüthrich *et al.*, 1982). Similarly, correlations between protein conformation and other n.m.r. parameters, for example chemical shifts and relaxation times, could then be investigated on a reliable basis. Finally, and perhaps most intriguing in view of biological interests, the resonance assignments provide a basis to extend the studies of internal flexibility of BPTI (Wagner & Wüthrich, 1979*a*; Wüthrich *et al.*, 1980) to cover essentially the entire molecular structure.

We thank Dr W. Braun, M. Billeter and G. Wider for stimulating discussions, and Mrs E. Huber and Mrs E. H. Hunziker for the careful preparation of the manuscript and the illustrations. Financial support was obtained from the Schweizerischer Nationalfonds (project 3.528.79) and by a special grant from Eidgenössische Technische Hochschule for the purchase of the 500 MHz spectrometer.

REFERENCES

Anil Kumar, Ernst, R. R. & Wüthrich, K. (1980*a*). *Biochem. Biophys. Res. Commun.* **95**, 1–6.
Anil Kumar, Wagner, G., Ernst, R. R. & Wüthrich, K. (1980*b*). *Biochem. Biophys. Res. Commun.* **96**, 1156–1163.
Anil Kumar, Wagner, G., Ernst, R. R. & Wüthrich, K. (1981). *J. Amer. Chem. Soc.* **103**, 3654–3658.
Aue, W. P., Bartholdi, E. & Ernst, R. R. (1976). *J. Chem. Phys.* **64**, 2229–2246.
Baumann, R., Wider, G., Ernst, R. R. & Wüthrich, K. (1981). *J. Magn. Reson.* **44**, 402–406.
Billeter, M., Braun, W. & Wüthrich, K. (1982). *J. Mol. Biol.* **155**, 321–346.
Bundi, A. & Wüthrich, K. (1979*a*). *Biopolymers*, **18**, 285–298.
Bundi, A. & Wüthrich, K. (1979*b*). *Biopolymers*, **18**, 299–312.
Dayhoff, M. O. (1972). Editor of *Atlas of Protein Sequence and Structure*, National Biomed. Res. Found., Washington.
Deisenhofer, J. & Steigemann, W. (1975). *Acta Crystallogr. sect. B*, **31**, 238–250.
De Marco, A., Wagner, G. & Wüthrich, K. (1977). *Biophys. Struct. Mech.* **3**, 303–315.
Dubs, A., Wagner, G. & Wüthrich, K. (1979). *Biochim. Biophys. Acta*, **577**, 177–194.
Gordon, S. L. & Wüthrich, K. (1978). *J. Amer. Chem. Soc.* **100**, 7094–7096.
Jeener, J., Meier, B. H., Bachmann, P. & Ernst, R. R. (1979). *J. Chem. Phys.* **71**, 4546–4553.
Kalinichenko, P. (1976). *Stud. Biophys.* **58**, 235–240.
Kalk, A. & Berendsen, H. J. C. (1976). *J. Magn. Reson.* **24**, 343–366.
Nagayama, K. & Wüthrich, K. (1981). *Eur. J. Biochem.* **114**, 365–374.

Nagayama, K., Wüthrich, K. & Ernst, R. R. (1979). *Biochem. Biophys. Res. Commun.* **90**, 305–311.
Nagayama, K., Anil Kumar, Wüthrich, K. & Ernst, R. R. (1980). *J. Magn. Res.* **40**, 321–334.
Noggle, J. H. & Schirmer, R. E. (1971). *The Nuclear Overhauser Effect*, Academic Press, New York.
Perkins, S. J. & Wüthrich, K. (1979). *Biochim. Biophys. Acta*, **576**, 409–423.
Richarz, R., Sehr, P., Wagner, G. & Wüthrich, K. (1979). *J. Mol. Biol.* **130**, 19–30.
Richarz, R., Nagayama, K. & Wüthrich, K. (1980). *Biochemistry*, **19**, 5189–5196.
Snyder, G. H., Rowan III, R., Karplus, S. & Sykes, B. D. (1975). *Biochemistry*, **14**, 3765–3777.
Solomon, I. (1955). *Phys. Rev.* **99**, 559–565.
Tschesche, H., (1974). *Angew. Chemie. Int. Ed. Engl.* **13**, 10–28.
Wagner, G. & Wüthrich, K. (1979*a*). *J. Mol. Biol.* **134**, 75–94.
Wagner, G. & Wüthrich, K. (1979*b*). *J. Magn. Reson.* **33**, 675–680.
Wagner, G., De Marco, A. & Wüthrich, K. (1976). *Biophys. Struct. Mech.*, **2**, 139–158.
Wagner, G., Wüthrich, K. & Tschesche, H. (1978*a*). *Eur. J. Biochem.* **86**, 67–76.
Wagner, G., Wüthrich, K. & Tschesche, H. (1978*b*). *Eur. J. Biochem.* **89**, 367–377.
Wagner, G., Anil Kumar & Wüthrich, K. (1981). *Eur. J. Biochem.* **114**, 375–384.
Wider, G., Lee, H. K. & Wüthrich, K. (1982). *J. Mol. Biol.* **155**, 367–388.
Wüthrich, K. (1976). *NMR in Biological Research: Peptides and Proteins*, North-Holland Publishing Company, Amsterdam.
Wüthrich, K. & Wagner, G. (1975). *FEBS Letters*, **50**, 265–268.
Wüthrich, K. & Wagner, G. (1979). *J. Mol. Biol.* **130**, 1–18.
Wüthrich, K., Wagner, G., Richarz, R. & Perkins, S. J. (1978). *Biochemistry*, **17**, 2253–2263.
Wüthrich, K., Wagner, G., Richarz, R. & Braun, W. (1980). *Biophys. J.* **10**, 549–560.
Wüthrich, K., Wider, G., Wagner, G. & Braun, W. (1982). *J. Mol. Biol.* **155**, 311–319.

Edited by S. Brenner